RSC Advances

PAPER

View Article Online
View Journal | View Issue

Check for updates

Cite this: *RSC Adv.*, 2021, **11**, 38293

Preparation of hollow tubular TpBD COF and pod-like ZIF-8/H-TpBD COF tubes using a porous anodic aluminum oxide membrane as template†

Jiayuan He,‡[a] Rijian Mo,‡[bc] Guangzheng Jiang,[a] Lei He,[c] Chunxia Zhou,[ab] Zhong-Ji Qian,[bc] Pengzhi Hong*[ab] and Chengyong Li *[bc]

Received 11th August 2021
Accepted 23rd November 2021

DOI: 10.1039/d1ra06062g

rsc.li/rsc-advances

By sacrificing a porous anodic aluminum oxide (AAO) membrane as a template, hollow tubular TpBD (H-TpBD) covalent organic framework (COF) tubes were synthesized *in situ* and zeolitic imidazolate framework (ZIF-8) nanoparticles were creatively synthesized *in situ* in H-TpBD tubes at room temperature. H-TpBD COF tubes and ZIF-8/H-TpBD COF tubes were procured by using a strong base or acid to remove the AAO membrane. Then they were analyzed by X-ray diffraction, Fourier infrared spectroscopy, scanning electron microscope, transmission electron microscope, *etc.* Surprisingly, the obtained TpBD COF has a very small aperture (1.8 nm), thinner tube thickness (50 nm), high stability, and a smooth and homogeneous surface. And the pod-like ZIF-8/H-TpBD COF with complete tubular structure was also obtained.

Open Access Article. Published on 29 November 2021. Downloaded on 2/12/2026 8:40:50 AM.
This article is licensed under a Creative Commons Attribution-NonCommercial 3.0 Unported Licence.

Covalent organic frameworks (COFs) are a class of crystalline organic porous materials formed by connecting organic units (consisting of light atoms such as C, H, O, and N) through chemical covalent bonds, and have atomically precise porous framework structures. COF polymers can be predesigned and synthesized by topology-diagram-directed polymer development.[1] The key to obtaining polymers with predesigned primary and higher-order structures is to fuse covalent bonds and non-covalent interactions into a polymer system to form a first-order structure with a specific structure or chain segment, thus guiding the formation of higher-order structures. The COF, with the covalent bond and non-covalent interaction in the polymerization system, has the characteristics of this kind of polymer. And in order to be suitable for a particular field, COF-derived materials can also be prepared by forming composites and high-temperature pyrolysis.[2] In addition, due to its unique characteristics, such as nano pore-size (usually ranging from several angstroms to several nanometers),[3] ordered channel structure, excellent thermal stability, and excellent chemical properties, COF has attracted great attention in many fields, including separation,[4] catalysis,[5,6] energy storage,[7] and medicine delivery.[8,9]

Some studies have found that COF with hollow nanostructures carry the characteristics of low density, high specific surface area, and strong load capacity. So hollow-structured COF materials have gained a lot of attention in recent years. And the hollow COF got broad application prospects in the fields of environmental protection,[10,11] biomedicine,[12,13] membrane separation,[14] and food safety.[15,16] Gole *et al.* reported a hollow imine COF tube formed by s bottom-up microtubular self-assembly, with a mean diameter of about 150 nm.[17] However, the machinability of conventional self-assembled COFs is very challenging. Without spatial and temporal control of the nucleation and growth, COFs are always separated into insoluble and cannot processable solids.[9] Huang *et al.* prepared hollow nanotubes by selectively hydrolyzing the target covalent bond in the two-dimensional hetero-pore COF.[18] Although it can be synthesized by self-assembly, by self-assembly, the synthesis of hollow structures by templates provides significant advantages in terms of size and shape control and freedom of template variability.[19] Hollow 1,3,5-triformylphloroglucinol/*p*-phenylenediamine (TpPa) COF nanostructures were synthesized with template-assisted method. ZnO@TpPa is formed with ZnO nanorods as the core, and then the ZnO nanorods are removed to obtain a hollow TpPa COF nanostructure, which has a capsule-like morphology. Nevertheless, the synthesis of nanosized low-density hollow COF tubes remains a challenge.[20]

Here, tubular and pod-like COF structures were synthesized using a porous anodic aluminum oxide (AAO) membrane as

[a]*College of Food Science and Technology, Guangdong Ocean University, Zhanjiang 524088, China*

[b]*Shenzhen Institute of Guangdong Ocean University, Shenzhen, Guangdong 518114, China. E-mail: hongpz@gdou.edu.cn; cyli@gdou.edu.cn*

[c]*School of Chemistry and Environment, Guangdong Ocean University, Zhanjiang 524088, China*

† Electronic supplementary information (ESI) available. See DOI: 10.1039/d1ra06062g

‡ These authors have contributed equally to this work and share first authorship.

© 2021 The Author(s). Published by the Royal Society of Chemistry

Open Access Article. Published on 29 November 2021. Downloaded on 2/12/2026 8:40:50 AM.
This article is licensed under a Creative Commons Attribution-NonCommercial 3.0 Unported Licence.

a template. AAO membrane was prepared subject to the literature prepared by a two-step anodic oxidation method and with a pore size of 200 nm.[21] The 1,3,5-triformylphloroglucinol (Tp) and benzidine (BD) were used as reaction solvents to form a TpBD COF tubular structure in AAO by *in situ* growth method. 3 M NaOH solution was used to remove the AAO membrane to obtain a hollow tubular TpBD COF that has the characteristics of rich hydrophilic groups and high stability[22] (Scheme 1(a), a more detailed explanation can be seen in the ESI†). Firstly, imines were formed on the template by continuous mutual conversion inter-conversion from enol to keto forms, and then the network tubular skeleton of polyimines was formed by precipitation polymerization of TP and BD under the condition of equilibrium control of the template. The obtained polymer is amorphous in structure, has inherent imine bonds and internal dynamic imine exchange process, which can initiate the structural transition from disorder to order.[23] Analogously, zeolitic imidazolate framework (ZIF-8, a highly porous crystalline solid based on the coordination of organic 2-methylimidazole (2-mIM) ligand and Zn^{2+} ionic subunit)[24] was formed in TpBD COF/AAO by *in situ* growth method using zinc nitrate and dimethylimidazole as reaction reagents. Finally, the pod-like structure of the ZIF-8/H-TpBD COF tube can be obtained by treatment with 20 μL of 1% hydrofluoric acid (HF) for 30 seconds and ultrasonication to remove AAO (Scheme 1(b), a more detailed explanation can be seen in the ESI†). The combination of ZIF-8 and COF tube is designed to better integrate the strengths of both sides. Meanwhile, contrasted with other methods, the size of the synthesized COF tube is adjustable using the AAO nanochannel as a template. With the AAO nanochannel as the template, the size of the synthesized COF tubes can be adjusted and a pod-like COF tube can be synthesized. This provides a new method for the synthesis of COF tubes.

The reaction time of Tp and BD plays an indispensable role in the synthesis of TpBD COF/AAO nanotubes. Fig. 1 and S1† reveal scanning electron microscope (SEM) images of TpBD/AAO synthesized at different reaction times (1–8 hours). When the reaction time of Tp and BD is fewer than 5 hours, almost no COF tube is formed in the AAO nanochannel. Remarkably, when the reaction time was extended to 5 hours in Fig. 1(e),

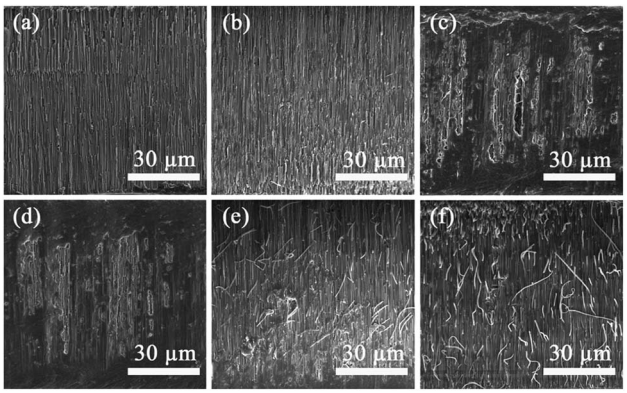

Fig. 1 SEM images of TpBD COF/AAO membrane synthesized by Tp and BD under different reaction times. (a) 1 h. (b) 2 h. (c) 3 h. (d) 4 h. (e) 5 h. (f) 6 h.

TpBD COF/AAO tubular structures started to mature in the AAO nanochannels. It shows that when the reaction time is 1–5 hours, it is the transition process of TpBD aggregation network structure from disorder to order. Furthermore, when the reaction time was extended from 5 to 8 hours (Fig. S1†), the shape of the COF nanotubes in the AAO nanochannels did not change with the increase of the reaction time, but grew along the vertical direction of the AAO membrane hole. And it extends outwards during growth, while preserving a complete tubular structure. Although it looks very disorderly. Obviously, the COF tubes grew along the pores of AAO membrane, namely, the AAO membrane is used as the template to extend to the direction of the pore channel to form nanotubes. Through comparison, it can be found that with the increase of reaction time, the number of COF tubes gradually reduced and the length of tubes also increased significantly (Fig. S1†).

FT-IR spectroscopy was used to characterize the prepared samples to verify the formation of TpBD COF/AAO tubes in the

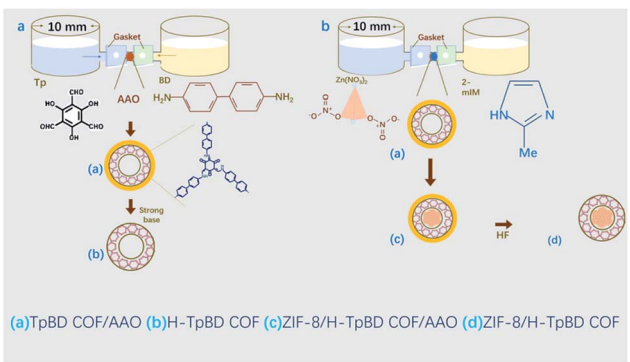

Scheme 1 Synthesis of H-TpBD COF nanotubes and ZIF-8/TpBD COF peapod composite. (a) H-TpBD COF nanotubes (b) ZIF-8-TpBD COF.

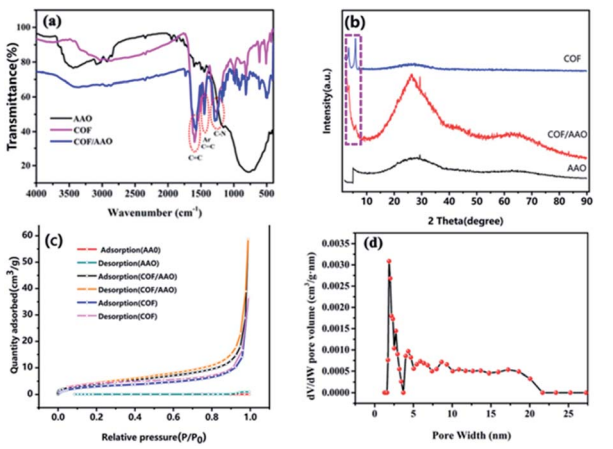

Fig. 2 Characterization of TpBD COF/AAO. (a) FT-IR spectra of H-TpBD COF nanotubes, TpBD COF/AAO and AAO. (b) XRD pattern of TpBD COF/AAO and AAO. (c) N_2 adsorption analyses of H-TpBD COF nanotubes, TpBD COF/AAO and AAO. (d) The pore size of TpBD COF nanotube.

© 2021 The Author(s). Published by the Royal Society of Chemistry

Open Access Article. Published on 29 November 2021. Downloaded on 2/12/2026 8:40:50 AM.
This article is licensed under a Creative Commons Attribution-NonCommercial 3.0 Unported Licence.

AAO membrane. As shown in Fig. 2(a), the TpBD COF/AAO have appeared characteristic peaks at 1595, 1465 and 1259 cm^{-1} correspond to the C=C, Ar (C=C), and C–N of the TpBD respectively. Which is consistent with the literature report. The spectrum showed that the C=N peak disappeared, and a new C=C peak appeared at 1595 cm^{-1},[25,26] illustrating the effectively formation of TpBD. Compared with pure AAO, at the wavenumber range of 500 to 4000 cm^{-1} that the infrared spectrum of TpBD COF/AAO has the same characteristic peaks (1595, 1465 and 1259 cm^{-1}) as TpBD COF. But there is no characteristic peak in pure AAO film, as shown in the Black Line in Fig. 2(a). The above analysis confirms that the TpBD COF/AAO has been successfully formed in nanochannels of AAO membrane. To eliminate internal stress and make the crystal structure of COF more uniform through grain reconstruction, TpBD nanotubes were annealed at 800 °C. As shown in Fig. 2(b), XRD spectrum of TpBD/AAO presents moderate crystallinity, exhibiting the first 2θ peak at low angles of 3.3°, corresponding to the (100) reflection plane.[22]

In order to evaluate the porosity of the as-synthesized TpBD COF nanotube, we have collected the N_2 adsorption isotherms of the AAO, TpBD COF/AAO and TpBD COF nanotube. As shown in Fig. 2(c), the N_2 adsorption analyses performed for TpBD COF/AAO, which is characteristic of microporous materials.[22,26] The surface area of TpBD COF nanotube, TpBD/AAO membrane and AAO membrane was calculated using the BET model. The increased surface area of H-TpBD COF nanotube (11.37 $m^2\ g^{-1}$) and TpBD COF/AAO (15.21 $m^2\ g^{-1}$) as compared to AAO (4.51 $m^2\ g^{-1}$) confirms the removal of AAO, leaving behind the TpBD COF nanotube. The pore size distribution of TpBD COF nanotube calculated related to the BET model shows that the pore size of TpBD COF nanotube is primarily clustered at 1.8 nm in Fig. 2(d).

In order to obtain the tubular TpBD COF structure, the AAO template must be removed from the TpBD COF/AAO. 5 M NaOH solution was exploited to remove AAO. Scanning electron microscope (SEM) and transmission electron microscope (TEM) were used to characterize the obtained TpBD COF tube, as shown in Fig. 3. Remarkably, the TpBD COF after removing the AAO is a tubular structure, and the tube length can be extended to 60 μm. Of course, the length of the COF tubes will be inconsistent due to the difference in reaction time or reaction position. In addition, most COF tubes are clustered together. After sonication, individual COF tubes or shorter COF tubes can be obtained (Fig. S2†). As shown in Fig. 3(c) and (d), it can be found that the COF tube is a hollow tube and its surface is smooth and uniform. The time and average diameter distribution diagram are shown in Fig. S3.† With the change of reaction time of TP and BD, the diameter of the synthetic COF tube also changes, and when the reaction time is 6 hours, the diameter reaches the maximum. Fig. S4† shows that the inner and outer diameter is mainly distributed at 160 nm and 211 nm, respectively. Hence the thickness of the tube wall is about 50 nm. After that, as the reaction time increases, the diameter of the tube gradually decreases after 8 hours. It may be due to the increase of tubular structure, which leads to the enhancement of the π–π stacking effect and restrict the extension of pipe diameter.

Furthermore, we also synthesized ZIF-8/H-TpBD COF that ZIF-8 are grew in the TpBD COF/AAO tube. The pod-like

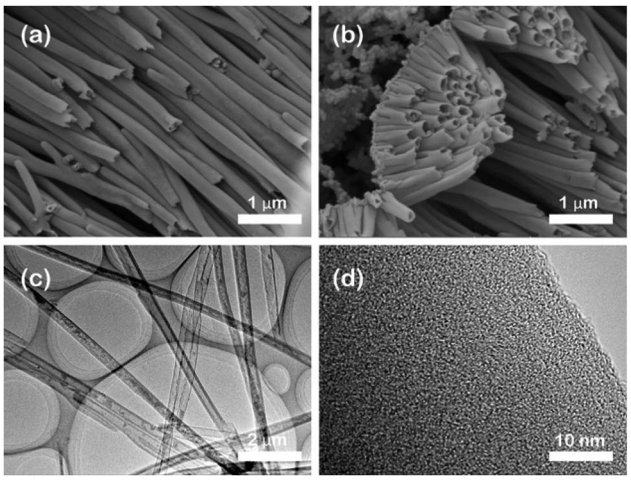

Fig. 3 Morphological characterization of TpBD COF nanotubes. (a) and (b) SEM images, (c) TEM image, and (d) HRTEM image of H-TpBD COF nanotubes.

structure of the ZIF-8/H-TpBD COF tube can be obtained by treatment with 20 μL of 1% hydrofluoric acid for 30 seconds and ultrasonication to remove AAO. Fig. 4 are the TEM images of ZIF-8/H-TpBD COF/AAO, including cross-section view and overview of ZIF-8 in the COF tube. It can be found that the COF tube is filled with ZIF-8 but still preserves a hollow tube structure, while the ZIF-8 is evenly distributed in the tube. Combining the ZIF-8 structure into the H-TpBD COF tube is an innovative idea in this article, which entirely utilizes the space of the COF tube. In order to verify the practicability of the synthetic materials, the adsorption of tetracycline in water by H-TpBD COF and ZIF-8/H-TpBD COF were performed. The adsorption capacity of H-TpBD COF and ZIF-8/H-TpBD COF are 2.97 mg mg^{-1} and 4.17 mg mg^{-1} (Fig. 5), respectively. Compared with the reference, the H-TpBD/COF and ZIF/H-TpBD/COF have the great potential application in environmental protection (a more detailed explanation can be seen in the ESI†).[27]

In summary, using porous AAO membrane as a template, we innovatively synthesized H-TpBD COF and the *in situ* generated pod-like ZIF-8 COF structures. The H-TpBD COF has an inner and outer diameter of 160 nm and 211 nm, and the ultrathin thickness of pipe of about 50 nm. The ZIF-8 particles are distributed in the tubular TpBD COF without damaging the integrity of the H-TpBD COF tubes. Combining ZIF-8 with COF with stable structure to better integrate the advantages of both

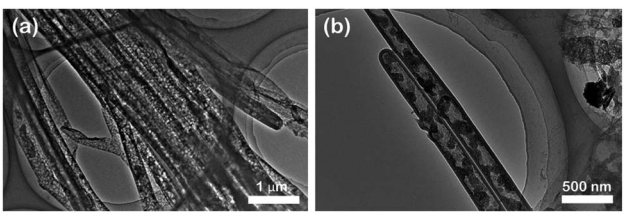

Fig. 4 TEM images of ZIF-8/H-TpBD COF/AAO. (a) sectional view. (b) ZIF-8 in the COF.

Open Access Article. Published on 29 November 2021. Downloaded on 2/12/2026 8:40:50 AM.
This article is licensed under a Creative Commons Attribution-NonCommercial 3.0 Unported Licence.

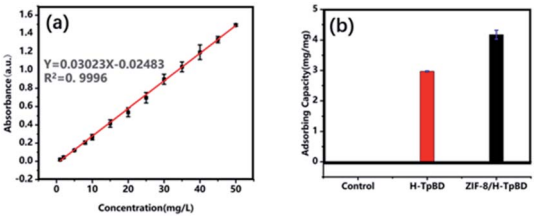

Fig. 5 (a) The linear range of tetracycline. (b) The adsorption capacity of tetracycline by H-TpBD COF and ZIF-8/H-TpBD COF.

parties is the latest highlight of this article. It is also believed that this will be one of the important directions for further research on polycrystalline polymer materials. These materials show great potential to be applied to the fields of separation, catalysis, environmental protection, and food safety.

Author contributions

Jiayuan He: conceptualization, writing–original draft, writing–review & editing. Rijian Mo: investigation, formal analysis. Guangzhneg Jiang: collect the samples. Lei He: collect the samples. Chunxia Zhou: collect the samples. Zhong-Ji Qian: investigation, formal analysis. Pengzhi Hong: conceptualization, funding acquisition. Chengyong Li: supervision, project administration, funding acquisition.

Conflicts of interest

The authors declare that they have no known competing financial interests or personal relationships that could have appeared to influence the work reported in this paper.

Acknowledgements

This work was supported by National Natural Science Foundation of China (21874029), Guangdong Basic and Applied Basic Research Foundation (2021A1515010291), Project of Enhancing School with Innovation of Guangdong Ocean University (2020ZDZX2029), Shenzhen Science and Technology R&D Fund (KCXFZ202002011011057), Special Funds for Science Technology Innovation and Industrial Development of Shenzhen Dapeng New District (KJYF202001-06, PT202001-18).

Notes and references

1 I. Ahmed and S. H. Jhung, *Coord. Chem. Rev.*, 2021, **441**, 213989.
2 K. Geng, V. Arumugam, H. Xu, Y. Gao and D. Jiang, *Prog. Polym. Sci.*, 2020, **108**, 8814–8933.
3 R.-R. Liang, A. Ru-Han, S.-Q. Xu, Q.-Y. Qi and X. Zhao, *J. Am. Chem. Soc.*, 2020, **142**, 70–74.
4 J. L. Fenton, D. W. Burke, D. Qian, M. O. de la Cruz and W. R. Dichtel, *J. Am. Chem. Soc.*, 2021, **143**, 1466–1473.
5 J.-C. Wang, C.-X. Liu, X. Kan, X.-W. Wu, J.-L. Kan and Y.-B. Dong, *Green Chem.*, 2020, **22**, 1150–1155.
6 G. C. Dubed Bandomo, S. S. Mondal, F. Franco, A. Bucci, V. Martin-Diaconescu, M. A. Ortuño, P. H. van Langevelde, A. Shafir, N. López and J. Lloret-Fillol, *ACS Catal.*, 2021, **11**, 7210–7222.
7 M. Yu, N. Chandrasekhar, R. K. M. Raghupathy, K. H. Ly, H. Zhang, E. Dmitrieva, C. Liang, X. Lu, T. D. Kuehne, H. Mirhosseini, I. M. Weidinger and X. Feng, *J. Am. Chem. Soc.*, 2020, **142**, 19570–19578.
8 L.-G. Ding, S. Wang, B.-J. Yao, F. Li, Y.-A. Li, G.-Y. Zhao and Y.-B. Dong, *Adv. Healthcare Mater.*, 2021, **10**, 2001821.
9 H. S. Sasmal, A. Halder, S. Kunjattu, K. Dey, A. Nadol, T. G. Ajithkumar, P. R. Bedadur and R. Banerjee, *J. Am. Chem. Soc.*, 2019, **141**, 20371–20379.
10 Y. Ying, A. M. Pourrahimi, Z. Sofer, S. Matejkova and M. Pumera, *ACS Nano*, 2019, **13**, 11477–11487.
11 L. Wang, Y. Yang, H. Liang, N. Wu, X. Peng, L. Wang and Y. Song, *J. Hazard. Mater.*, 2021, **409**, 124528.
12 M. Li, S. Qiao, Y. Zheng, Y. H. Andaloussi, X. Li, Z. Zhang, A. Li, P. Cheng, S. Ma and Y. Chen, *J. Am. Chem. Soc.*, 2020, **142**, 6675–6681.
13 T. Huo, Y. Yang, M. Qian, H. Jiang, Y. Du, X. Zhang, Y. Xie and R. Huang, *Biomaterials*, 2020, **260**, 120305.
14 Y. Liu, H. Wu, S. Wu, S. Song, Z. Guo, Y. Ren, R. Zhao, L. Yang, Y. Wu and Z. Jiang, *J. Membr. Sci.*, 2021, **618**, 118693.
15 X.-X. Wang, L. Liu, X.-L. Wang, G.-J. Xu, R.-S. Zhao, M.-L. Wang, J.-M. Lin and X. Wang, *Food Chem.*, 2021, **361**, 130018.
16 Y. Lu, Y. Liang, Y. Zhao, M. Xia, X. Liu, T. Shen, L. Feng, N. Yuan and Q. Chen, *ACS Appl. Mater. Interfaces*, 2021, **13**, 1644–1650.
17 B. Gole, V. Stepanenko, S. Rager, M. Gruene, D. D. Medina, T. Bein, F. Wuerthner and F. Beuerle, *Angew. Chem., Int. Ed.*, 2018, **57**, 846–850.
18 L. Huang, L. Ao, W. Wang, D. Hu, Z. Sheng and W. Su, *Chem. Commun.*, 2015, **51**, 3923–3926.
19 G. Das, T. Skorjanc, S. K. Sharma, F. Gandara, M. Lusi, D. S. S. Rao, S. Vimala, S. K. Prasad, J. Raya, D. S. Han, R. Jagannathan, J.-C. Olsen and A. Trabolsi, *J. Am. Chem. Soc.*, 2017, **139**, 9558–9565.
20 P. Pachfule, S. Kandmabeth, A. Mallick and R. Banerjee, *Chem. Commun.*, 2015, **51**, 11717–11720.
21 R. Mo, L. He, C. Zhou, Z.-J. Qian, P. Hong, S. Sun, Z. Wang, Y. Wang and C. Li, *Anal. Chem.*, 2019, **91**, 8184–8191.
22 H. Yang, X. Cheng, X. Cheng, F. Pan, H. Wu, G. Liu, Y. Song, X. Cao and Z. Jiang, *J. Membr. Sci.*, 2018, **565**, 331–341.
23 J. Tan, S. Namuangruk, W. Kong, N. Kungwan, J. Guo and C. Wang, *Angew. Chem., Int. Ed.*, 2016, **55**, 13979–13984.
24 S. K. Alsaiari, S. S. Qutub, S. Sun, W. Baslyman, M. Aldehaiman, M. Alyami, A. Almalik, R. Halwani, J. Merzaban, Z. Mao and N. M. Khashab, *Sci. Adv.*, 2021, **7**, eabe7174.
25 C.-X. Yang, C. Liu, Y.-M. Cao and X.-P. Yan, *Chem. Commun.*, 2015, **51**, 12254–12257.
26 B. P. Biswal, S. Chandra, S. Kandambeth, B. Lukose, T. Heine and R. Banerjee, *J. Am. Chem. Soc.*, 2013, **135**, 5328–5331.
27 H. R. Nodeh and H. Sereshti, *RSC Adv.*, 2016, **6**, 89953–89965.

© 2021 The Author(s). Published by the Royal Society of Chemistry